Federal Aviation Administration

ANALYSIS OF THE RISK OF AN AIRBUS A380 HAND FLOWN BALKED LANDING PENETRATING THE ICAO CODE E OFZ

Branch Study Report
AFS-440-BSR-02
March 2005

Flight Systems Laboratory

NOTICE

This document is disseminated under the sponsorship of the U.S. Department of Transportation in the interest of information exchange. The United States Government assumes no liability for the contents or use thereof.

The United States Government does not endorse products or manufacturers. Trade or manufacturers' names appear herein solely because they are considered essential to the objective of this report.

Executive Summary

The purpose of this study is to determine the probability of penetration of the ICAO Annex 14 Code E OFZ (Inner Transitional Surface) by an A380 during a hand-flown balked landing operation.

In the ICAO Annex 14 to the Convention of International Civil Aviation, the OFZ is specified to have a base width (Inner Approach Surface) of 120 meters for Code E aircraft and a base width of 155 meters for Code F aircraft (see Figure 1). In both cases the Inner Transitional Surface forms a plane sloping away from the base at 33.3%.

The study is intended to determine the risk of the A380, a Code F aircraft, penetrating the Code E OFZ during a hand-flown (flight director assisted) balked landing operation under typical environmental conditions.

The study applies extreme value analysis, a type of statistical analysis, to determine the penetration probability. The results of this analysis show that the probability of penetration is on the order of one in one billion (1 in 1,000,000,000). Specifically, the most conservative assumptions lead to an upper bound for this probability of penetration of 8.6 in 1,000,000,000.

TABLE OF CONTENTS

1.0	Introduction	1
2.0	Test Plan	2
3.0	Test Results	2
4.0	Analysis	3
5.0	Conclusion	15
Appendix		18

LIST OF ILLUSTRATIONS

Tables

Table 1	Test Crosswind Distribution	2
Table 2	Go Around Rates	4
Table 3	Wind Distributions: Actual versus Test	6
Table 4	Wind Speed by category	12
Table 5	Probabilities by Wind Category	12
Table 6	Probabilities by Height Category	12
Table 7	Penetration Probability Scenario Results	15

Figures

Figure 1	OFZ Code E and Code F Surfaces	1
Figure 2	"S" Related to Wind and Initiation Height	5
Figure 3	Wind Distributions: Actual versus Test	6
Figure 4	GEV Density Function Graph	8
Figure 5	Probability Using Density Graph	9
Figure 6	Three Scenario Densities Graphs	11
Figure 7	GEVALL Density Function Graph	13
Figure 8	Alternate Approach Graphs	17

1.0 Introduction

The purpose of this study is to determine the probability of penetration of the ICAO Annex 14 Code E OFZ (Inner Transitional Surface) by an A380 during a hand-flown balked landing operation.

In the ICAO Annex 14 to the Convention of International Civil Aviation, the OFZ is specified to have a base width (Inner Approach Surface) of 120 meters for Code E aircraft and a base width of 155 meters for Code F aircraft (see Figure 1). In both cases the Inner Transitional Surface forms a plane sloping away from the base at 33.3%.

The study is intended to determine the risk of the A380, a Code F aircraft, penetrating the Code E OFZ during a hand-flown (flight director assisted) balked landing operation under typical environmental conditions.

Figure 1

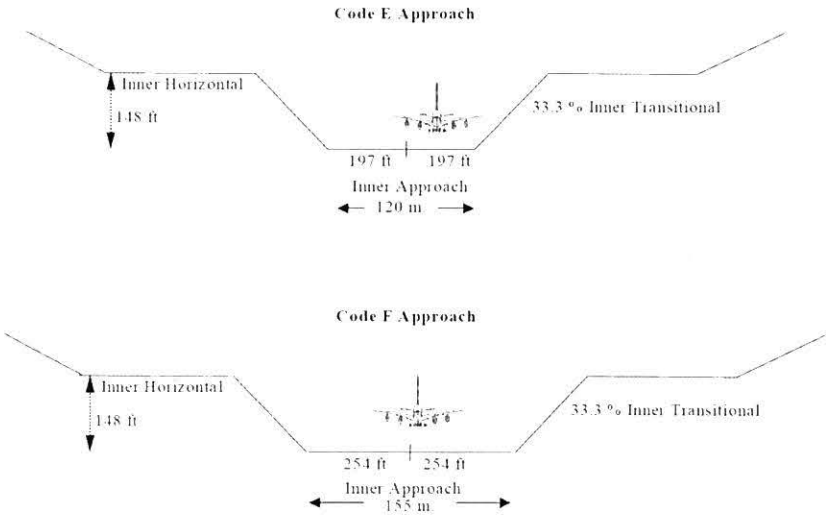

2.0 Test Plan

In order to determine the probability of penetration of the Code E OFZ we performed a series of tests of the balked landing operation using Airbus simulators in Toulouse and Berlin. These tests were designed to simulate the conditions of an Airbus A380 balked landing operation as closely as possible.

We performed 156 operational runs in Toulouse and 356 runs in Berlin all with professional flight crews. Of those 512 runs, 333 were hand flown balked landing operations (the other 179 were either actual landings or autopilot operations).

We had reason to believe that extreme crosswind conditions and very low balked landing initiation heights would increase the probability of OFZ penetration, so we included a disproportionate number of those cases in the test plan. The proportion of runs by crosswind speed and balked landing initiation height is indicated in Table 1.

Table 1

Initiation	Crosswind (knots)						
Height (ft)	0	10	18	21	23	25	Total
10	4%	8%	13%	2%	0%	6%	34%
40	3%	9%	8%	2%	6%	6%	35%
70	3%	8%	11%	0%	6%	3%	31%
Total	10%	26%	32%	5%	12%	15%	100%

For each run we measured aircraft position and orientation variables 15 times per second in order to determine the relationship between the A380 wing tips and the Code E Inner Transitional Surface.

3.0 Test Results

Since the Code E Inner Transitional Surface is a sloping surface, the relationship between the A380 wing tip and the surface varies by height even if the wing tip does not deviate laterally. For this reason, we normalized the measure of the distance from the wing tip to the OFZ surface. To do this, we defined a variable (called S) whose value is the percent lateral deviation of the wing tip between its nominal position and the Code E Inner Transitional Surface. That is, S is the actual wing tip deviation from nominal divided by the possible wing tip deviation, where *possible* means the distance from the wing tip to the surface when the aircraft is on track in the nominal position. For example, if the aircraft's lateral deviation from the nominal track is 0, the value of S is 0%. If the aircraft's left (or right) wing tip is touching the surface, the value of S is 100%. If the wing tip is exactly half way between nominal position and the surface, the value of S is 50%.

We calculated values for S for each data point along the aircraft's track starting with the initiation of the balked landing (taken to be when the throttle angle first exceeds 50°) and ending when the aircraft's lower wing tip has exceeded the 45 meter height of the sloping

Inner Transitional Surface (where the surface becomes horizontal) on its balked landing ascent. We then determined the maximum S value for each of the 333 balked landing runs.

For analysis purposes the variables of interest from the test data for each run are then: the maximum S value for the run, the crosswind speed, and the planned height at which the balked landing was initiated. A table of these values for the 333 runs is included in Appendix A.

4.0 Analysis

Risk is the combination of

- the consequence (or severity) of a Hazard Event and the
- probability of its occurring within the Scenario of interest.

The purpose of the present study is to determine the probability component of the risk of the Hazard Event: an A380 wing tip penetrates the ICAO Code E OFZ at least once during a Scenario operation.

Analysis Preliminaries

Here we establish five preliminary results that we will use in the analysis proper. First, we ensure that the Toulouse and Berlin data does not need to be analyzed separately. Second, we establish a reasonable estimate for balked landings. Third, we validate that crosswind speed and balked landing initiation height really do affect the value of S as we had suspected. Fourth, we compare the crosswind speeds used in the test with typical representative crosswind speeds to establish that test crosswind speeds are not representative. And finally, we compare the distribution of balked landing initiation heights used in the test with typical initiation heights to establish that test initiation heights are not representative.

1. Toulouse and Berlin data should not be separated for analysis:

We performed both a Kolmogorov-Smirnov test and a Two-Sample Chi-Square test on the Toulouse and Berlin data to determine if they can be said to represent different distributions. The null hypothesis for each test was: the two sets of data represent the same distribution. The results of the two tests were consistent: each indicates that the null hypothesis should not be rejected. That is, there is no reason to separate the data for analysis since they appear to represent a single distribution.

2. The balked landing rate to use is less than 1.9 per 1000 landing attempts:

We compared Go-Around rates available from five European airports and from a sample of runway 14R at Chicago O'Hare airport (see Table 2). These rates are consistently around 1.9 Go-Arounds per 100 attempted landings. However, while every balked landing is a Go-Around, not all Go-Arounds are balked landings.

And since we have no data for actual balked landing rates, we use the Go-Around rate as an upper bound. Anecdotal information indicates that the balked landing rate may be on the order of one-tenth the Go-Around rate.

Table 2

Go Around Rates

Airport	Year	Approaches	GA	GA per approach	Approaches/GA
LFPG	2003	257475	691	2.68E-03	373
LFPO	2003	103248	150	1.45E-03	688
LEBL	2002	135268	200	1.48E-03	676
LEBL	2003	140275	237	1.69E-03	592
LEMD	2002	183727	279	1.52E-03	659
LEMD	2003	189173	369	1.95E-03	513
LEPA	2002	80305	145	1.81E-03	554
LEPA	2003	84387	139	1.65E-03	607
TOTAL		**1173858**	**2210**	**1.88E-03**	**531**
KORD	**1998-2000**	**43960**	**84**	**1.91E-03**	**523**

3. Crosswind and balked landing initiation height affect S:

In developing the test plan we believed that crosswind speed would have a significant effect on lateral deviation from the nominal track (measured by variable S) and that balked landing initiation height would have a significant effect (the lower the initiation height the greater the lateral deviation).

Figure 2 shows the graphical relationships among the three variables: S, Crosswind Speed, and Initiation Height. The colored surface is a smoothed surface created from the S means at each x-wind/height combination. The small circles represent actual S values at those x-wind/height coordinates.

The obvious conclusion from this data is that both higher crosswind speed and lower initiation height lead to greater S values. (S values are plotted in the vertical axis in Figure 2.)

Figure 2

Berlin & Toulouse
s related to x-wind & balk initiation height

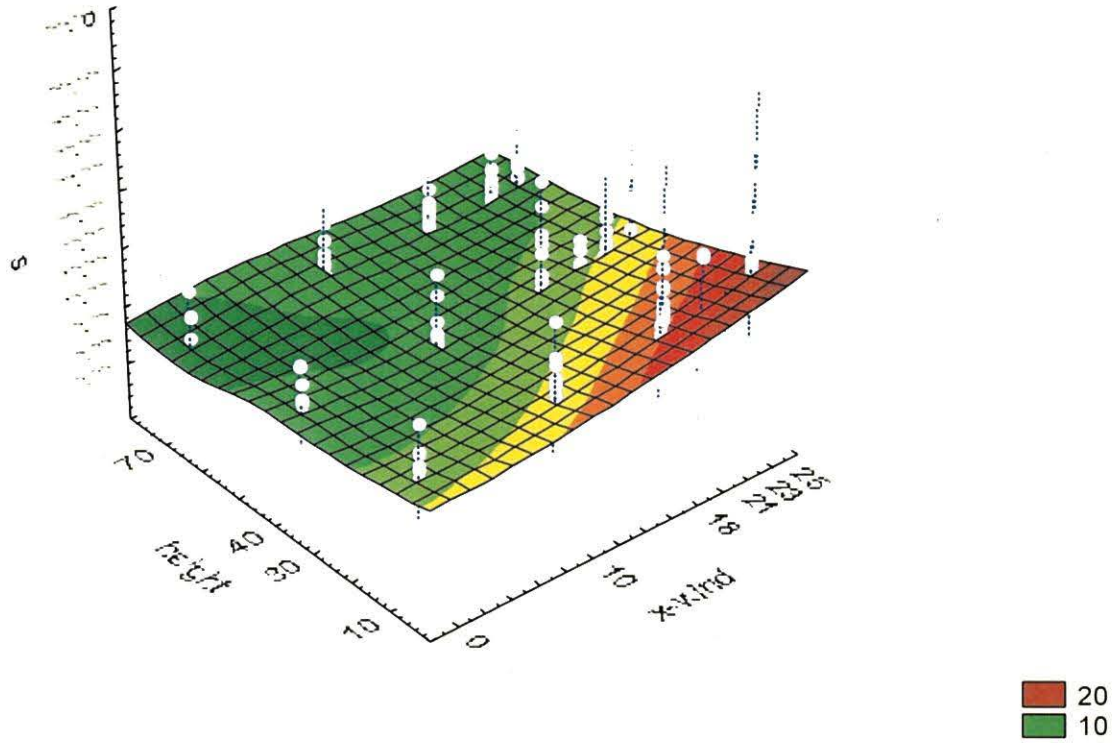

4. Crosswind speeds used in the test are not representative:

Since we believed that higher crosswind speeds would affect lateral deviations (S), we included many more high wind speed runs in the test than would be typical in an actual airport operational environment. We did this to help us understand the relationship between crosswind speed and balked landing lateral deviation.

The analysis must therefore compensate for this imbalance by using an actual crosswind speed distribution, comparing it to the test distribution. The distribution we use as actual is from the table in Figure A4-7 of Appendix 4 to AC 120-28D. Table 3 lists the corresponding test and actual distribution values.

Table 3

Speed	Test	Actual
0-5	10	55
5-10	13	30
10-15	13	10
15-20	32	4.5
20-25	32	0.5

And Figure 3 displays the same information graphically. Note that the test wind value of 10 knots represented 26% of the values and is divided between the 5-10 and 10-15 categories here giving 13% in each for a balanced comparison.

Figure 3

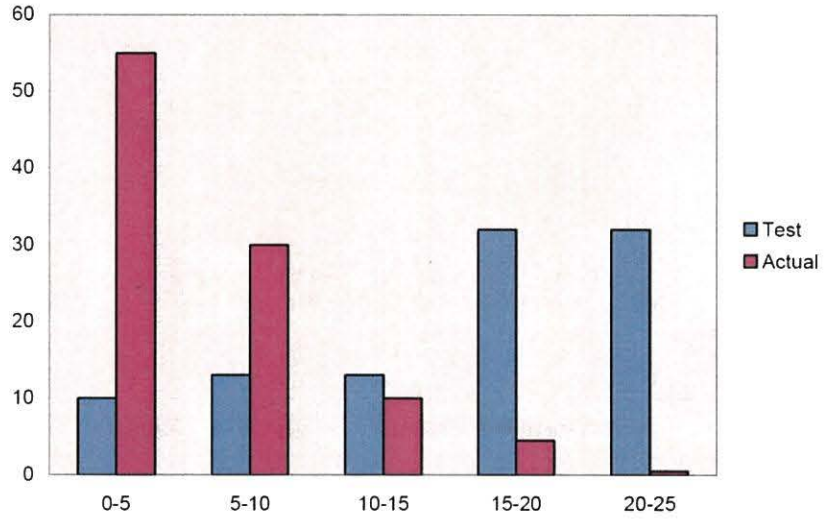

5. Distribution of balked landings by initiation height is not representative:

There are currently no reliable data available to this study that demonstrate the distribution of balked landings by initiation height. The FAA AFS-420 Chicago O'Hare Land and Hold Short study data indicate that almost all go-arounds are initiated above 70 feet (about 97%) and that certainly far less than 10% of them are initiated below 15 feet. But the very small sample size of go-arounds at low altitudes in this data (combined with the fact that these are go-arounds and not specifically balked landings) prevents us from using them to find accurate distributions for balked landings initiated below 70 feet.

Probability of OFZ Penetration

To calculate the probability that an A380 wingtip penetrates the Code E OFZ (Inner Transitional Surface) we use a three step methodology.

- First, we establish the Scenario of Interest. This is the scenario to which the probability applies. And it includes attribute assumptions such as crosswind distribution, initiation height distribution, and type of landing.
- Second, we use the data (See Appendix A) to develop a distribution of maximum S values for the Scenario of Interest.
- And third, we use this distribution to estimate probability that S > 100%, that is, that a wing tip penetrates the Code E OFZ surface under the Scenario of Interest.

Scenario 1 (artificial crosswinds, artificial initiation heights)

1. Establish Scenario 1

In this scenario we assume the actual crosswind and initiation height distributions are the same as those used in the 333 test runs. We must emphasize that this is an artificial assumption based on the relationship between the actual crosswind speeds and those used in the test (see Analysis Preliminary 4 above) and the relationship between the (less well understood) apparent actual initiation height distribution and those used in the test (see Analysis Preliminary 5 above).

Since (a) the proportion of both higher crosswind speeds and lower initiation heights in the test is much higher than in actual conditions and (b) the relationship between those two variables and the variable S is such that higher crosswind speeds and lower initiation heights are directly related to higher values of S (see Analysis Preliminary 3), then we would expect this scenario to lead to a higher probability of OFZ penetration than one using actual conditions.

Assumptions:

- A hand-flown balked landing has occurred, as in the test.
- Crosswind speeds are those of the test (not actual distributions)
- Balked landing initiation heights are those of the test (not actual distributions)

2. Develop a Distribution for Maximum S for Scenario 1

Next, we use classical Extreme Value Theory to develop a distribution for the maximum S values. This theory provides the two things. First, it provides a family of distributions (called GEV, or General Extreme Value distributions) that model block maximums such as those of the variable S. Second, it provides the justification for using a GEV distribution to extrapolate beyond the range of the maximum S values found in the test data.

The family of GEV distributions is described by the distribution function:

$\mathrm{GEV}(x) = \exp\left\{-\left[1+\xi\left(\frac{x-\mu}{\sigma}\right)\right]^{-1/\xi}\right\}$, where μ is the location parameter, σ is the scale parameter, and ξ is the shape parameter. Changing the value of any one of the parameters provides a different member of the family of GEV distributions.

We use the test data and a standard extreme value technique (extreme value maximum likelihood estimation) to estimate the three parameter values and thus the specific distribution that fits our data.

For this scenario, the parameter values the estimation technique yields are: $\mu = 6.336$, $\sigma = 3.677$, and $\xi = 0.075$ with standard errors 0.227, 0.169, and 0.040, respectively.

The density function corresponding to GEV(x) with these parameters is plotted in Figure 4.

Figure 4

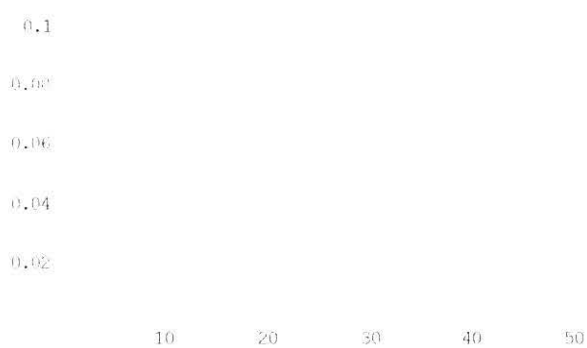

Appendix B contains graphical justification for the level of fit in the form of probability, quantile, and density plots.

3. Estimate the probability that S > 100% for Scenario 1

We estimate the probability that S > 100%, given that a hand-flown balked landing has been attempted under this scenario by calculating the area under the GEV density function to the right of 100 (See Figure 5). This area is 6.7 E-07 (meaning, 6.7 multiplied by 10 to the negative seventh power) with a standard error of 1.9 E-06. Thus, P(S > 100%) = 6.7 E-07 ± 1.9 E-06, given this scenario: that a hand-flown balked landing has occurred and the test crosswind and initiation height conditions are used. This estimate is likely high due to the use of the artificially high crosswind distribution and artificially low initiation height distribution. However, it does provide an upper bound estimate for the actual

OFZ penetration probability. A 95% confidence interval estimate for this upper bound is 6.7 E-07 ± 3.8 E-06.

Figure 5

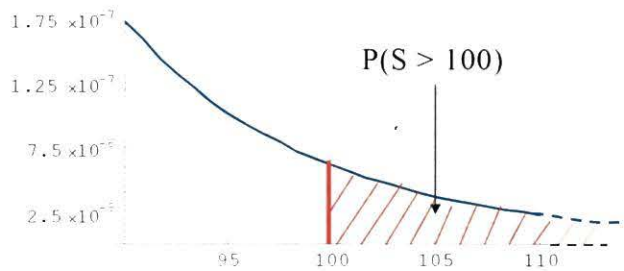

Scenario 2 (actual crosswinds, artificial initiation heights)

1. Establish Scenario 2

In this scenario we assume the actual initiation height distribution is the same as that used in the 333 test runs, but that the crosswind distribution is the actual distribution given in Analysis Preliminary 4 above. Again, we must emphasize that, while the crosswind situation represents actual conditions, the test initiation height distribution we are using is an artificial assumption.

And since (a) the proportion of lower initiation heights in the test is much greater than in actual conditions and (b) the relationship between this variable and the variable S is such that lower initiation heights are directly related to higher values of S (see Analysis Preliminary 3), then we would expect this scenario (as with Scenario 1) to lead to a higher probability of OFZ penetration than one using actual conditions.

Assumptions:

- A hand-flown balked landing has occurred, as in the test.
- Crosswind speeds follow the actual distribution (not the test distribution)
- Balked landing initiation heights are those of the test (not actual)

2. Develop a Distribution for Maximum S for Scenario 2

Next, we use classical Extreme Value Theory as in Scenario 1, except now we develop three distributions of the maximum S values: one for each of three categories of crosswind speeds.

These three categories are based on the crosswind speed values 0 – 10, 10-20, and 20-25 knots. Where the first category includes the 0 and 10 knot runs (it has 120 runs), the second category includes the 18 knot runs (108 runs), and the last category includes the 21, 23, and 25 knot runs (105 runs). We chose these particular categories because the cutoff speeds are typical, the number of runs per category are similar, and the data within each category is homogeneous.

Next we develop three GEV distributions, one for each crosswind category.

The distribution for the first category, which we will call GEV1, has parameters $\mu = 5.307$, $\sigma = 3.372$, and $\xi = -0.024$ with standard errors 0.354, 0.260, and 0.078, respectively.

The distribution for the second category, GEV2, has parameters $\mu = 6.851$, $\sigma = 3.654$, and $\xi = 0.081$ with standard errors 0.399, 0.299, and 0.074, respectively.

The distribution for the third category, GEV3, has parameters $\mu = 7.147$, $\sigma = 3.547$, and $\xi = 0.1923$ with standard errors 0.395, 0.314, and 0.083, respectively.

Figure 6 shows plots of these three distributions' density functions: GEV1 is the left-most, dotted-blue curve, GEV2 is the next solid red curve, and GEV3 is the dashed curve that begins below the GEV2 curve.

Figure 6

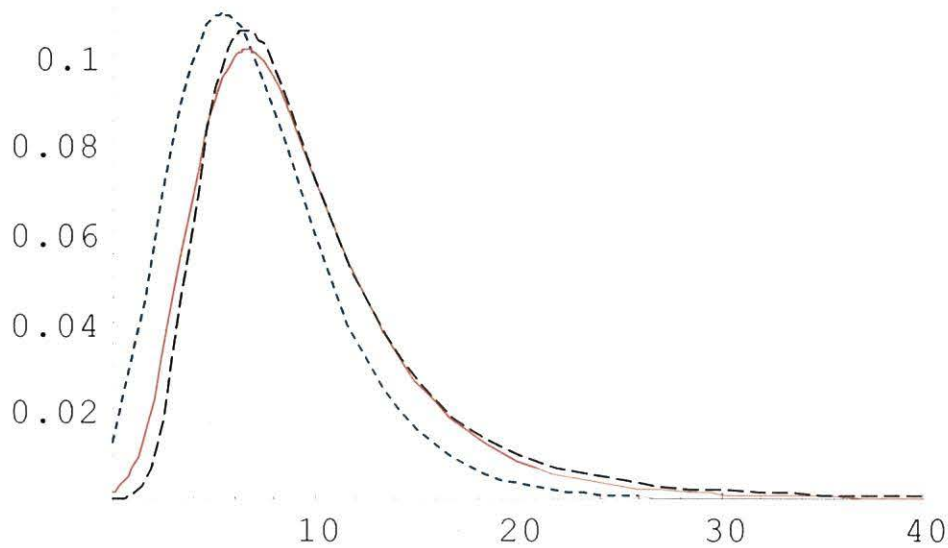

3. Estimate the probability that S > 100% for Scenario 2

We estimate the probability that S > 100%, given that a hand-flown balked landing has been attempted under this scenario by calculating the area under each GEV density function (GEV1, GEV2, and GEV3) to the right of 100 and multiplying each of these areas by the likelihood of encountering a crosswind of that category.

This yields a mixed distribution, GEVALL based on the three GEV distributions and the crosswind likelihoods for each category (see Table 4):

$$\text{GEVALL}(x) = 0.850\text{GEV1}(x) + 0.145\text{GEV2}(x) + 0.005\text{GEV3}(x).$$

Table 4

5 Category Speed	Actual %	3 Category Speed	Actual %
0-5	55		
5-10	30	0-10	85
10-15	10		
15-20	4.5	10-20	14.5
20-25	0.5	20-25	0.5

The calculations are summarized in Table 5 below.

Table 5

Wind Category Speed	Wind Category Actual %	GEV	P(S>100)	Actual % Times P(S>100)
0-10	85	GEV1	0.0 E-14	0.0 E-07
10-20	14.5	GEV2	9.7 E-07	1.4 E-07
20-25	0.5	GEV3	8.7 E-05	4.4 E-07
All	100	GEVALL		5.8 E-07

Thus, P(S > 100%) = 5.8 E-07 with a standard error of 1.2 E-06, given this scenario: that a hand-flown balked landing has occurred and the actual crosswind and artificial (test) initiation height conditions are used. A 95% confidence interval estimate for this upper bound is 5.8 E-07 ± 2.4 E-06. Again, this estimate is surely high due to the use of the artificially low initiation height distribution. But since the actual crosswind distribution was used (as opposed to the artificially high test conditions used in Scenario 1) the estimate here in Scenario 2 (5.8 E-07) is somewhat smaller than that of Scenario 1 (6.7 E-07), and in addition provides a validation in that the values are reasonably close.

Figure 7 shows the plot of the mixed GEVALL(x) density function.

Figure 7

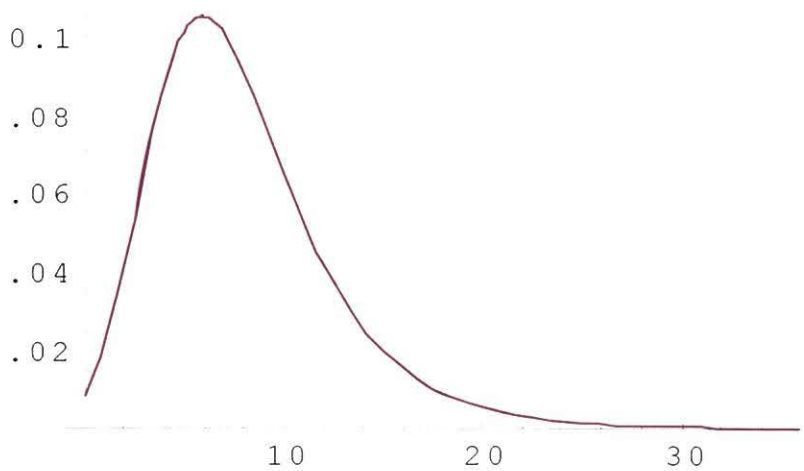

Scenario 3 (artificial crosswinds, actual initiation heights)

1. Establish Scenario 3

In this scenario we assume the crosswind distribution is that of the artificial test conditions and we use the rough assumption for the balked landing initiation height distribution given above in Analysis Preliminary 5. As indicated there, we currently have no accurate distribution of balked landings by initiation height, but

we can estimate that the proportion of balked landings initiated below 15 feet is less than 10%.

And since (a) the proportion of high crosswinds in the test is much greater than in actual conditions and (b) the relationship between this variable and the variable S is such that higher crosswind speeds are directly related to higher vales of S (see Analysis Preliminary 3), then we would expect this scenario (as with Scenarios 1 and 2) to lead to a higher probability of OFZ penetration than one using actual conditions.

Assumptions:

- A hand-flown balked landing has occurred, as in the test.
- Crosswind speeds follow the test distribution
- Balked landing initiation heights are closer to the actual distribution

2. Develop a Distribution for Maximum S for Scenario 3

Next, we use classical Extreme Value Theory as in Scenarios 1 and 2, except now we develop two distributions for the maximum S values: one for each of two categories of initiation heights (below 15 feet and above 15 feet).

The first category includes the 10 foot initiation heights (it has 113 runs), the second category includes 40 and 70 foot initiation heights (220 runs).

Next we develop two GEV distributions, one for each height category.

The distribution for the first category, which we will call GEVA, has parameters $\mu = 8.299$, $\sigma = 4.511$, and $\xi = 0.032$ with standard errors 0.469, 0.337, and 0.058, respectively.

The distribution for the seçond category, GEVB, has parameters $\mu = 5.600$, $\sigma = 3.145$, and $\xi = 0.050$ with standard errors 0.238, 0.176, and 0.049, respectively.

3. Estimate the probability that S > 100% for Scenario 3

We estimate the probability that S > 100%, given that a hand-flown balked landing has been attempted under this scenario by calculating the area under each GEV density function (GEVA and GEVB) to the right of 100 and multiplying each of these areas by the likelihood of encountering a crosswind of that category.

This yields a mixed distribution, GEVBOTH based on the two GEV distributions and the initiation height likelihoods for each category:

$$\text{GEVBOTH}(x) = 0.10\text{GEVA}(x) + 0.90\text{GEVB}(x).$$

The calculations are summarized in Table 6 below.

Table 6

Height Category	Height Category Actual %	GEV	P(S>100)	Actual % Times P(S>100)
Below 15	10	GEVA	1.55 E-07	1.6 E-08
Above 15	90	GEVB	1.13 E-08	1.0 E-08
Both	100	GEVBOTH		2.6 E-08

Thus, P(S > 100%) = 2.6 E-08 with a standard error of 1.1 E-07, given this scenario: that a hand-flown balked landing has occurred and the artificial (test) crosswind and estimated actual initiation height conditions are used. A 95% confidence interval estimate for this upper bound is 2.6 E-08 ± 1.1 E-07. Again, this estimate is likely high due to the use of the artificially high crosswind distribution. It does, however, provide a check on the previous two estimates: it is lower than both, as would be expected, and it is reasonably close to their values.

5.0 Conclusion

It would be possible to analyze a fourth scenario with assumptions for actual crosswind and initiation height distributions. However, we do not attempt that analysis for three reasons. First, if we categorized the data by both crosswind and height the number of runs in each category would be small. Second, we would need to make assumptions about the relationship between the crosswind speed and height variables (such as independence) that may be unwarranted. And third, we do not have an accurate distribution of balked landings by initiation height as it is.

Based on the three scenarios analyzed, we can, however, calculate a reasonable upper bound on the probability of ICAO Code E OFZ penetration. Table 7 summarizes the probability estimates from the three scenarios. It is important to recall that these are conditional probabilities. That is, they are probabilities of OFZ penetration given that a hand-flow balked landing has occurred. We must factor in the probability of a hand-flown balked landing occurring to complete the calculation.

Table 7

Scenario	Penetration Probability*
1	6.7 E-07
2	5.8 E-07
3	2.6 E-08

*Given hand-flow balked landing.

Each of these probabilities was developed using assumptions that would tend to produce higher rather than lower values. They differ primarily because of the variations in the sets of runs used to fit the various distributions.

To calculate a reliable upper bound on the OFZ penetration probability, we make these further assumptions:

1. Use the greatest of the three scenario probabilities (6.7 E-07).
2. Use the balked landing rate of Analysis Preliminary 2, which is actually an upper bound of 1.9 balked landings per 1000 landing attempts.
3. Focus only on OFZ penetrations due to balked landings, assuming that normal landing produce effectively no penetrations.

The probability of hand-flown A380 ICAO OFZ penetration during a balked landing (OFZP) is given by:

P(OFZP) = P(Balk)•P(OFZP | Balk) + P(no Balk) •P(OFZP|no Balk).

Which reduces to: P(OFZP) = P(Balk)•P(OFZP | Balk), since P(OFZP|no Balk) is effectively zero. That is, no Balk (i.e., normal landings) produce effectively zero penetrations by assumption 3 above.

Since, P(OFZP | Balk) < 6.7 E-07, by assumption 1 above.
And, P(Balk) < 1.9 E-03, by assumption 2 above.

Then, P(OFZP) < 1.3 E-09.

That is, an estimate of an upper bound for the probability of an A380 ICAO Code E OFZ penetration during a hand-flown balked landing is determined to be 1.3 E-09.

An even more conservative assumption would be to use the upper end of the 95% confidence interval for the penetration probability. So that instead of using a penetration probability of 6.7 E-07, we use 4.5 E-06. This would lead to an estimate of an upper bound for the probability of an A380 ICAO Code E OFZ penetration during a hand-flown balked of 8.6 E-09.

Note that we developed this estimate using several assumptions, each of which would tend to produce a higher value rather than a lower one. So we may conclude that this estimate is a reliable upper bound on the actual probability.

Addendum to the Conclusion

The results above for penetration probability have been validated by a slightly different approach to probability estimation. Instead of estimating the probability of the variable S exceeding 100%, we examine the relationship between the value of S and the height of

the critical wing tip (h). Using this perspective we generate iso-probability curves for various values of probabilities.

In the graphs below (Figure 8) we use probabilities of p = 0.99999 and p = 0.999999. The corresponding curves are where the probability of S exceeding the curve boundaries are 1.0 E-05 and 1.0 E-06 respectively. Multiplying these probabilities by the probability of a balked landing (P(BALK) = 1.9 E-03) yields probabilities for penetration above the curves between 1.9 E-08 and 1.9 E-09.

Iso-probability Curve for S as a Function of Wing Tip Height (h) with Probability, p = 0.99999

Iso-probability Curve for S as a Function of Wing Tip Height (h) with Probability, p = 0.999999

Figure 8

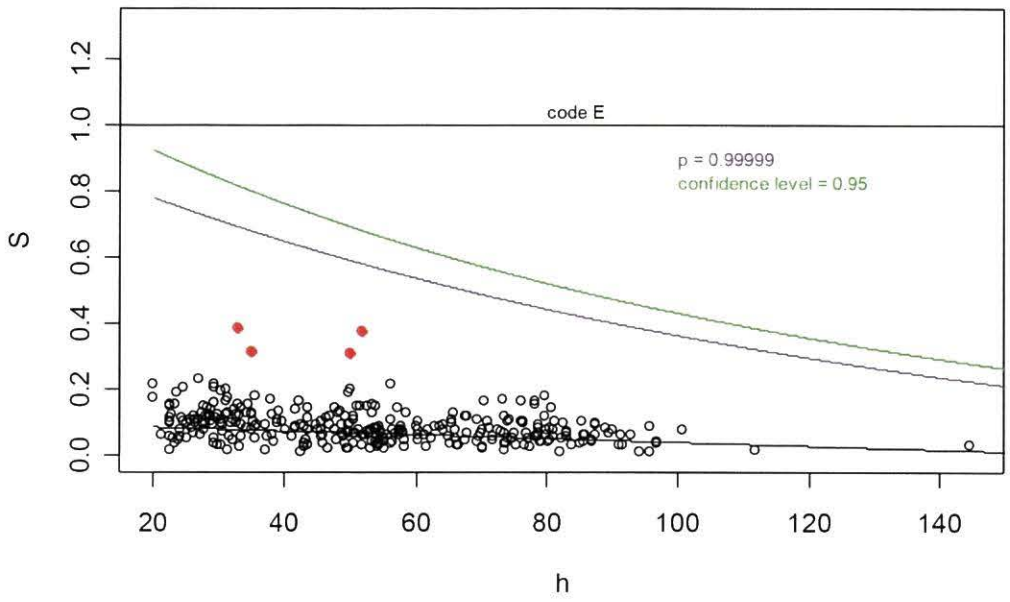
code E
p = 0.99999
confidence level = 0.95
S
h
0.0
0.2
0.4
0.6
0.8
1.0
1.2
20
40
60
80
100
120
140

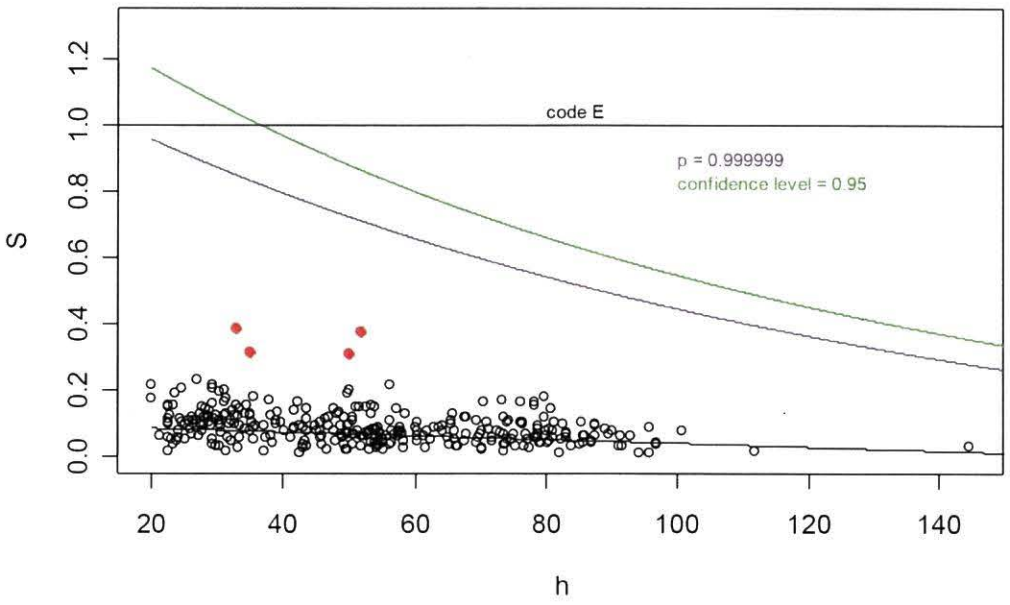
code E
p = 0.999999
confidence level = 0.95
S
h
0.0
0.2
0.4
0.6
0.8
1.0
1.2
20
40
60
80
100
120
140

Appendix A

Test Data Summary for 333 Runs

Location	Date	Scenario	Height (ft)	Crosswind (kts)	S Max (%)
Berlin	23-Aug-04	2	10	10	11.63
Berlin	23-Aug-04	3	10	18	9.65
Berlin	23-Aug-04	4	10	25	31.26
Berlin	23-Aug-04	5	40	0	8.00
Berlin	23-Aug-04	6	40	10	6.16
Berlin	23-Aug-04	7	40	25	19.63
Berlin	23-Aug-04	8	70	10	5.58
Berlin	23-Aug-04	9	70	18	3.99
Berlin	23-Aug-04	10	70	25	14.36
Berlin	23-Aug-04	17	10	0	10.94
Berlin	23-Aug-04	19	10	10	10.90
Berlin	23-Aug-04	20	10	18	9.94
Berlin	23-Aug-04	21	10	25	3.26
Berlin	23-Aug-04	22	40	10	6.20
Berlin	23-Aug-04	23	40	18	14.84
Berlin	23-Aug-04	25	40	25	3.62
Berlin	23-Aug-04	26	70	0	2.52
Berlin	23-Aug-04	27	70	10	6.24
Berlin	23-Aug-04	29	70	18	11.54
Berlin	24-Aug-04	2	10	10	9.50
Berlin	24-Aug-04	3	10	18	12.18
Berlin	24-Aug-04	4	10	25	16.11
Berlin	24-Aug-04	5	40	0	3.22
Berlin	24-Aug-04	6	40	10	5.66
Berlin	24-Aug-04	6.2	40	10	6.54
Berlin	24-Aug-04	7	40	25	14.51
Berlin	24-Aug-04	8	70	10	5.19
Berlin	24-Aug-04	9	70	18	6.13
Berlin	24-Aug-04	10	70	25	7.58
Berlin	24-Aug-04	17	10	0	11.96
Berlin	24-Aug-04	19	10	10	11.66
Berlin	24-Aug-04	20	10	18	10.73
Berlin	24-Aug-04	21	10	25	9.29
Berlin	24-Aug-04	22	40	10	3.90
Berlin	24-Aug-04	23	40	18	15.03
Berlin	24-Aug-04	25	40	25	6.41
Berlin	24-Aug-04	26	70	0	2.25
Berlin	24-Aug-04	27	70	10	7.79
Berlin	24-Aug-04	29	70	18	6.46
Berlin	25-Aug-04	2	10	10	10.90
Berlin	25-Aug-04	3	10	18	14.14
Berlin	25-Aug-04	4	10	25	11.97
Berlin	25-Aug-04	5	40	0	14.47
Berlin	25-Aug-04	6	40	10	4.12
Berlin	25-Aug-04	7	40	25	10.62

Berlin	25-Aug-04	8	70	10	5.93
Berlin	25-Aug-04	9	70	18	7.77
Berlin	25-Aug-04	10	70	25	6.37
Berlin	25-Aug-04	17	10	0	10.39
Berlin	25-Aug-04	17.2	10	0	15.36
Berlin	25-Aug-04	19	10	10	12.62
Berlin	25-Aug-04	20	10	18	11.27
Berlin	25-Aug-04	21	10	25	20.87
Berlin	25-Aug-04	22	40	10	1.90
Berlin	25-Aug-04	23	40	18	12.41
Berlin	25-Aug-04	25	40	25	2.54
Berlin	25-Aug-04	26	70	0	5.56
Berlin	25-Aug-04	27	70	10	7.81
Berlin	25-Aug-04	29	70	18	1.78
Berlin	26-Aug-04	2	10	10	3.58
Berlin	26-Aug-04	3	10	18	20.17
Berlin	26-Aug-04	4	10	25	23.02
Berlin	26-Aug-04	5	40	0	6.97
Berlin	26-Aug-04	6	40	10	2.74
Berlin	26-Aug-04	6.2	40	10	14.86
Berlin	26-Aug-04	7	40	25	18.57
Berlin	26-Aug-04	8	70	10	17.76
Berlin	26-Aug-04	9	70	18	9.31
Berlin	26-Aug-04	10	70	25	9.82
Berlin	26-Aug-04	17	10	0	2.71
Berlin	26-Aug-04	19	10	10	9.55
Berlin	26-Aug-04	20	10	18	18.93
Berlin	26-Aug-04	21	10	25	37.29
Berlin	26-Aug-04	22	40	10	6.20
Berlin	26-Aug-04	23	40	18	19.62
Berlin	26-Aug-04	25	40	25	7.26
Berlin	26-Aug-04	26	70	0	8.94
Berlin	26-Aug-04	27	70	10	12.45
Berlin	26-Aug-04	29	70	18	4.79
Berlin	27-Aug-04	2	10	10	9.01
Berlin	27-Aug-04	3	10	18	9.75
Berlin	27-Aug-04	4	10	25	14.90
Berlin	27-Aug-04	5	40	0	12.79
Berlin	27-Aug-04	6	40	10	5.36
Berlin	27-Aug-04	7	40	25	6.47
Berlin	27-Aug-04	8	70	10	16.32
Berlin	27-Aug-04	9	70	18	6.43
Berlin	27-Aug-04	10	70	25	16.13
Berlin	27-Aug-04	17	10	0	5.41
Berlin	27-Aug-04	17.2	10	0	7.67
Berlin	27-Aug-04	19	10	10	10.75
Berlin	27-Aug-04	20	10	18	10.47
Berlin	27-Aug-04	21	10	25	13.01

Berlin	27-Aug-04	22	40	10	1.63
Berlin	27-Aug-04	23	40	18	5.99
Berlin	27-Aug-04	25	40	25	5.70
Berlin	27-Aug-04	26	70	0	7.56
Berlin	27-Aug-04	27	70	10	11.53
Berlin	27-Aug-04	29	70	18	4.38
Berlin	30-Aug-04	2	10	10	7.27
Berlin	30-Aug-04	3	10	18	6.06
Berlin	30-Aug-04	4	10	25	13.62
Berlin	30-Aug-04	5	40	0	7.27
Berlin	30-Aug-04	6	40	10	13.92
Berlin	30-Aug-04	7	40	25	13.29
Berlin	30-Aug-04	8	70	10	4.37
Berlin	30-Aug-04	9	70	18	7.45
Berlin	30-Aug-04	10	70	25	5.06
Berlin	30-Aug-04	17	10	0	9.79
Berlin	30-Aug-04	17.2	10	0	8.24
Berlin	30-Aug-04	19	10	10	9.22
Berlin	30-Aug-04	20	10	18	7.41
Berlin	30-Aug-04	21	10	25	14.70
Berlin	30-Aug-04	22	40	10	5.50
Berlin	30-Aug-04	23	40	18	4.22
Berlin	30-Aug-04	25	40	25	7.56
Berlin	30-Aug-04	26	70	0	6.18
Berlin	30-Aug-04	27	70	10	5.60
Berlin	30-Aug-04	29	70	18	7.88
Berlin	31-Aug-04	2	10	10	20.48
Berlin	31-Aug-04	3	10	18	12.60
Berlin	31-Aug-04	4	10	25	6.19
Berlin	31-Aug-04	5	40	0	11.35
Berlin	31-Aug-04	6	40	10	2.91
Berlin	31-Aug-04	7	40	25	5.37
Berlin	31-Aug-04	8	70	10	3.84
Berlin	31-Aug-04	9	70	18	3.91
Berlin	31-Aug-04	10	70	25	5.87
Berlin	31-Aug-04	17	10	0	5.54
Berlin	31-Aug-04	17.2	10	0	1.24
Berlin	31-Aug-04	19	10	10	10.21
Berlin	31-Aug-04	20	10	18	21.58
Berlin	31-Aug-04	21	10	25	15.62
Berlin	31-Aug-04	22	40	10	2.35
Berlin	31-Aug-04	23	40	18	10.45
Berlin	31-Aug-04	25	40	25	9.19
Berlin	31-Aug-04	26	70	0	3.54
Berlin	31-Aug-04	27	70	10	4.34
Berlin	31-Aug-04	29	70	18	2.54
Berlin	1-Sep-04	2	10	10	5.42
Berlin	1-Sep-04	3	10	18	38.18

Berlin	1-Sep-04	4	10	25	4.89
Berlin	1-Sep-04	5	40	0	6.23
Berlin	1-Sep-04	6	40	10	3.72
Berlin	1-Sep-04	6.2	40	10	6.69
Berlin	1-Sep-04	7	40	25	14.04
Berlin	1-Sep-04	8	70	10	4.80
Berlin	1-Sep-04	9	70	18	10.24
Berlin	1-Sep-04	10	70	25	7.43
Berlin	1-Sep-04	17	10	0	9.90
Berlin	1-Sep-04	19	10	10	4.63
Berlin	1-Sep-04	20	10	18	11.89
Berlin	1-Sep-04	21	10	25	19.08
Berlin	1-Sep-04	22	40	10	3.25
Berlin	1-Sep-04	23	40	18	6.12
Berlin	1-Sep-04	25	40	25	7.75
Berlin	1-Sep-04	26	70	0	10.70
Berlin	1-Sep-04	27	70	10	5.64
Berlin	1-Sep-04	29	70	18	6.48
Berlin	2-Sep-04	2	10	10	10.45
Berlin	2-Sep-04	3	10	18	8.79
Berlin	2-Sep-04	4	10	25	17.19
Berlin	2-Sep-04	5	40	0	0.77
Berlin	2-Sep-04	6	40	10	7.46
Berlin	2-Sep-04	6.2	40	10	4.41
Berlin	2-Sep-04	7	40	25	12.30
Berlin	2-Sep-04	8	70	10	7.63
Berlin	2-Sep-04	9	70	18	7.16
Berlin	2-Sep-04	10	70	25	10.44
Berlin	2-Sep-04	17	10	0	2.68
Berlin	2-Sep-04	19	10	10	7.25
Berlin	2-Sep-04	20	10	18	5.28
Berlin	2-Sep-04	21	10	25	10.02
Berlin	2-Sep-04	22	40	10	9.03
Berlin	2-Sep-04	23	40	18	11.59
Berlin	2-Sep-04	25	40	25	30.36
Berlin	2-Sep-04	26	70	0	1.80
Berlin	2-Sep-04	27	70	10	3.54
Berlin	2-Sep-04	29	70	18	6.10
Berlin	3-Sep-04	2	10	10	1.15
Berlin	3-Sep-04	3	10	18	8.13
Berlin	3-Sep-04	4	10	25	7.18
Berlin	3-Sep-04	5	40	0	3.11
Berlin	3-Sep-04	6	40	10	0.20
Berlin	3-Sep-04	6.2	40	10	6.21
Berlin	3-Sep-04	7	40	25	4.09
Berlin	3-Sep-04	8	70	10	5.79
Berlin	3-Sep-04	9	70	18	4.65
Berlin	3-Sep-04	10	70	25	5.63

Berlin	3-Sep-04	17	10	0	1.53
Berlin	3-Sep-04	19	10	10	4.90
Berlin	3-Sep-04	20	10	18	11.22
Berlin	3-Sep-04	21	10	25	7.62
Berlin	3-Sep-04	22	40	10	7.11
Berlin	3-Sep-04	23	40	18	4.39
Berlin	3-Sep-04	25	40	25	7.13
Berlin	3-Sep-04	26	70	0	2.71
Berlin	3-Sep-04	27	70	10	1.26
Berlin	3-Sep-04	29	70	18	6.47
Toulouse	21-May-04	2.1	40	18	13.28
Toulouse	21-May-04	3.1	70	23	2.62
Toulouse	21-May-04	3.2	70	23	9.77
Toulouse	21-May-04	4.1	10	10	5.85
Toulouse	21-May-04	6.1	40	23	14.16
Toulouse	21-May-04	7.1	10	18	2.93
Toulouse	21-May-04	8.1	70	18	5.92
Toulouse	21-May-04	9.1	70	10	0.89
Toulouse	21-May-04	12.1	40	23	8.88
Toulouse	21-May-04	13.1	10	18	7.43
Toulouse	21-May-04	14.1	70	23	4.02
Toulouse	21-May-04	17.1	10	23	7.10
Toulouse	4-Jun-04	2	40	18	19.25
Toulouse	4-Jun-04	3	70	23	12.74
Toulouse	4-Jun-04	4	10	18	8.12
Toulouse	4-Jun-04	5	10	21	3.33
Toulouse	4-Jun-04	8	70	18	10.05
Toulouse	4-Jun-04	9	40	21	7.35
Toulouse	4-Jun-04	11	40	23	11.78
Toulouse	4-Jun-04	12	10	18	11.07
Toulouse	4-Jun-04	15	70	18	1.93
Toulouse	4-Jun-04	16	40	18	3.83
Toulouse	7-Jun-04	2	40	18	8.47
Toulouse	7-Jun-04	3	70	23	8.74
Toulouse	7-Jun-04	4	10	18	11.14
Toulouse	7-Jun-04	7	40	23	9.32
Toulouse	7-Jun-04	8	70	18	6.01
Toulouse	7-Jun-04	11	40	23	9.88
Toulouse	7-Jun-04	12	10	18	9.88
Toulouse	7-Jun-04	13	70	23	7.42
Toulouse	7-Jun-04	15	40	18	8.38
Toulouse	7-Jun-04	17	10	10	12.35
Toulouse	7-Jun-04	18	40	10	6.07
Toulouse	7-Jun-04	19	70	10	7.80
Toulouse	18-Jun-04	2	40	18	7.05
Toulouse	18-Jun-04	3	70	23	2.91
Toulouse	18-Jun-04	4	10	18	14.71
Toulouse	18-Jun-04	5	10	21	9.71

Toulouse	18-Jun-04	7	40	23	6.14
Toulouse	18-Jun-04	9	40	21	7.97
Toulouse	18-Jun-04	11	40	23	7.20
Toulouse	18-Jun-04	12	10	18	6.27
Toulouse	18-Jun-04	13	70	23	4.37
Toulouse	18-Jun-04	15	70	18	3.97
Toulouse	18-Jun-04	16	40	18	4.00
Toulouse	18-Jun-04	17	10	10	6.24
Toulouse	1-Jul-04	2	70	23	8.97
Toulouse	1-Jul-04	3	40	18	9.90
Toulouse	1-Jul-04	4	10	18	5.23
Toulouse	1-Jul-04	6	10	21	4.67
Toulouse	1-Jul-04	7	40	23	5.19
Toulouse	1-Jul-04	8	70	18	10.23
Toulouse	1-Jul-04	11	40	23	14.48
Toulouse	1-Jul-04	12	10	18	11.74
Toulouse	1-Jul-04	13	70	23	4.91
Toulouse	1-Jul-04	15	70	18	3.57
Toulouse	1-Jul-04	16	40	18	2.08
Toulouse	6-Jul-04	2	70	23	10.19
Toulouse	6-Jul-04	3	40	18	8.77
Toulouse	6-Jul-04	4.1	10	18	13.22
Toulouse	6-Jul-04	4.2	10	18	22.46
Toulouse	6-Jul-04	6	10	21	9.97
Toulouse	6-Jul-04	7	40	23	6.43
Toulouse	6-Jul-04	8	70	18	6.64
Toulouse	6-Jul-04	9	40	21	10.22
Toulouse	6-Jul-04	11	40	23	5.84
Toulouse	6-Jul-04	12	10	18	18.10
Toulouse	6-Jul-04	13	70	23	7.95
Toulouse	6-Jul-04	15	70	18	3.36
Toulouse	6-Jul-04	16	40	18	2.83
Toulouse	6-Jul-04	17	10	10	15.41
Toulouse	6-Jul-04	18	40	10	1.84
Toulouse	6-Jul-04	19	70	10	5.23
Toulouse	16-Jul-04	2	70	23	6.73
Toulouse	16-Jul-04	3	40	18	8.29
Toulouse	16-Jul-04	4	10	18	16.83
Toulouse	16-Jul-04	6	10	21	7.80
Toulouse	16-Jul-04	7	40	23	7.93
Toulouse	16-Jul-04	8	70	18	4.27
Toulouse	16-Jul-04	9	40	21	14.02
Toulouse	16-Jul-04	11	40	23	10.67
Toulouse	16-Jul-04	12	10	18	12.14
Toulouse	16-Jul-04	13	70	23	3.88
Toulouse	16-Jul-04	15	40	18	11.81
Toulouse	16-Jul-04	16	70	18	15.74
Toulouse	16-Jul-04	17	10	10	7.44

Toulouse	16-Jul-04	18	40	10	7.97
Toulouse	16-Jul-04	19	70	10	10.52
Toulouse	20-Jul-04	2	70	23	7.26
Toulouse	20-Jul-04	3	40	18	3.09
Toulouse	20-Jul-04	4	10	18	7.35
Toulouse	20-Jul-04	6	10	21	7.01
Toulouse	20-Jul-04	7	40	23	4.00
Toulouse	20-Jul-04	8	70	18	6.69
Toulouse	20-Jul-04	9	40	21	6.69
Toulouse	20-Jul-04	11	40	23	8.35
Toulouse	20-Jul-04	12	10	18	12.55
Toulouse	20-Jul-04	13	70	23	2.97
Toulouse	20-Jul-04	15	40	18	9.65
Toulouse	20-Jul-04	16	70	18	3.79
Toulouse	20-Jul-04	17	10	10	14.03
Toulouse	20-Jul-04	18	40	10	3.88
Toulouse	20-Jul-04	19	70	10	3.24
Toulouse	22-Jul-04	2	70	23	8.23
Toulouse	22-Jul-04	3	40	18	8.70
Toulouse	22-Jul-04	4	10	18	9.53
Toulouse	22-Jul-04	6	10	21	15.91
Toulouse	22-Jul-04	7	40	23	8.93
Toulouse	22-Jul-04	8	70	18	7.95
Toulouse	22-Jul-04	9	40	21	11.71
Toulouse	22-Jul-04	11	40	23	21.76
Toulouse	22-Jul-04	12	10	18	14.48
Toulouse	22-Jul-04	13	70	23	6.10
Toulouse	22-Jul-04	15	40	18	8.88
Toulouse	22-Jul-04	16	70	18	8.88
Toulouse	22-Jul-04	17	10	10	4.61
Toulouse	22-Jul-04	18	40	10	8.49
Toulouse	22-Jul-04	19	70	10	16.63
Toulouse	26-Jul-04	2	70	23	6.26
Toulouse	26-Jul-04	3	40	18	10.57
Toulouse	26-Jul-04	4	10	18	10.32
Toulouse	26-Jul-04	6	10	21	15.30
Toulouse	26-Jul-04	7	40	23	6.34
Toulouse	26-Jul-04	8	70	18	5.02
Toulouse	26-Jul-04	9	40	21	9.25
Toulouse	26-Jul-04	11	40	23	5.58
Toulouse	26-Jul-04	12	10	18	14.28
Toulouse	26-Jul-04	12.1	10	18	10.11
Toulouse	26-Jul-04	13	70	23	10.16
Toulouse	26-Jul-04	15	40	18	6.63
Toulouse	26-Jul-04	16	70	18	3.27
Toulouse	26-Jul-04	17	10	10	9.57
Toulouse	26-Jul-04	18	40	10	6.48
Toulouse	26-Jul-04	19	70	10	16.96

Appendix B

Graphical evidence of fit for the Scenario 1 GEV distribution.

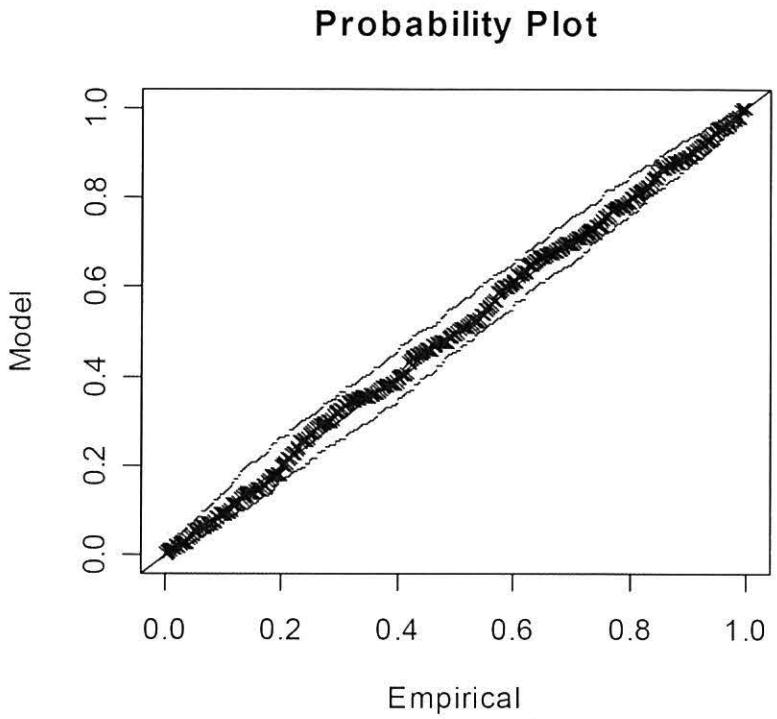

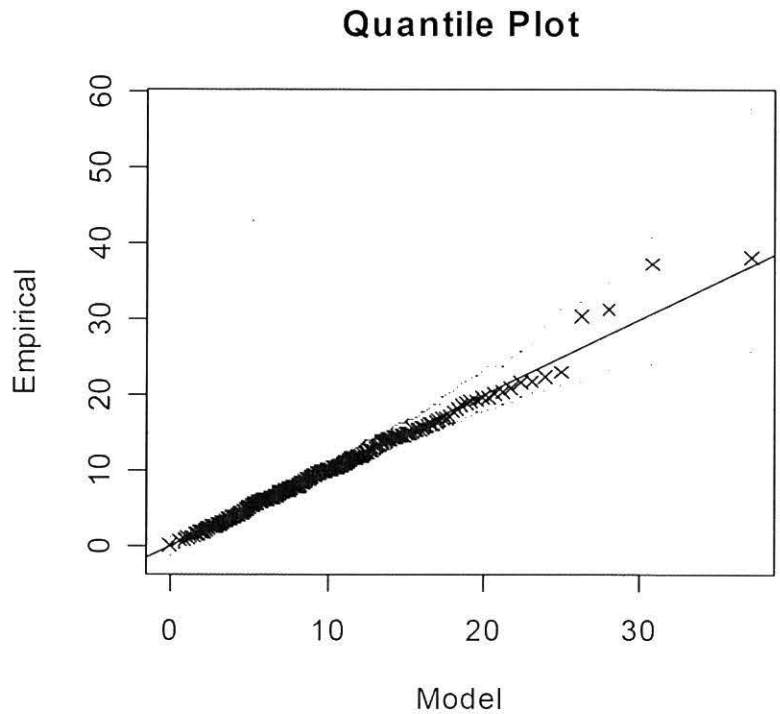
Quantile Plot
Empirical
0
10
20
30
40
50
60
0
10
20
30
Model

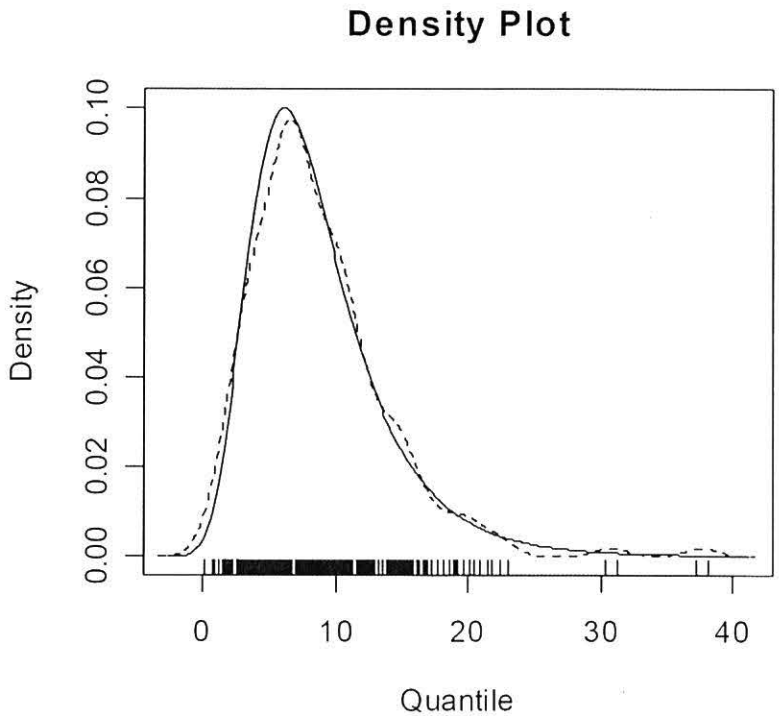
Density Plot
Density
0.00
0.02
0.04
0.06
0.08
0.10
0
10
20
30
40
Quantile